Effect of Impeller Blade Height on the Drop Size Distribution in Agitated Dispersions

By *Hani Naseef, Asem Soultan,* and *Michael Stamatoudis*

DOI: 10.1002/ceat.200500128

A common method to achieve a contact of two liquid phases – required for many chemical engineering operations – is the dispersion of one into the other by mechanical agitation. The drop size distribution in such an agitated dispersion is a result of the dynamic equilibrium existing between the breaking and coalescing drops. A comparison has been made of drop diameters produced by four disk type impellers differing only in blade height (D_W = 1, 2, 4 and 6 cm). Measurements in situ at 200, 250, 300, 350, 400, 450 rpm and at holdup fractions 0.02, 0.05, and 0.07, showed that the Sauter mean drop diameters increased up to 140 % as the impeller blade height decreased from 6 to 1 cm. Plots of $\ln a_{32}$ vs. $\ln N$, $\ln a_{32}$ vs. $\ln D_T$ and $\ln a_{32}$ vs. $\ln a_{max}$ gave straight lines.

1 Introduction

Many chemical engineering operations require the contact of two liquid phases. This contact expedites the heat and/or mass transfer between the two liquid phases. A common method to achieve this contact is the dispersion of one of the phases into the other by mechanical agitation. A review of this important area has been given by Tavlarides and Stamatoudis [1].

The drop size distribution in an agitated dispersion is a result of the dynamic equilibrium that exists between the breaking and coalescing drops. Decreasing the drop breakage rate or increasing the drop coalescence rate results in greater drops. Conversely, increasing the drop breakage rate or decreasing the drop coalescence rate results in smaller drop sizes. A mathematical model of this dynamic state can be obtained using population balances equations. The maximum stable drop in a turbulent field depends on the turbulent field itself and on the force that holds the drops together. Kolmogoroff [2] and Hinze [3] assumed that in order for a drop to become unstable and break, the kinetic energy of the drop oscillations must be sufficient to overcome the surface force holding the drop together. Thus, the Weber number, N_{We}, which is defined as the ratio of the kinetic energy to the surface energy, has a critical value above which the drop becomes unstable. In locally isotropic turbulent flows[1]:

$$(N_{We})_{crit} = \frac{c\rho_c \varepsilon^{2/3} a_{max}^{5/3}}{\sigma} = \text{constant} \quad (1)$$

where c is a constant, ρ_c is the continuous phase density, ε is the rate of energy dissipating per unit mass of the liquid, a_{max} is the maximum stable drop in the dispersion and σ is the interfacial tension. The maximum stable drop that can exist can be obtained from Eq. (1) and for a given system is:

$$a_{max} \propto \varepsilon^{-2/5} \quad (2)$$

The interfacial area that results from agitation depends on many parameters such as the geometry of the vessel and the impeller, the rotational speed, the physicochemical properties of the two liquids, and the holdup fraction of the dispersed phase. Several researchers [4–7] have found that the size of drops in an agitated vessel varies depending on the distance from the impeller region, where breakage predominates, and the circulation region, where coalescence is the main processes. In addition, Daglas and Stamatoudis [8] found that there is an influence of impeller vertical position on drop sizes ranging from a Sauter mean diameter decrease of 7.8 % to an increase of 35 % relative to the values obtained with the impeller at the center of the vessel.

While a lot of work has been done in the past on studying agitated dispersions, relatively little attention has been given to the effect of the geometry of the impeller on the drop size produced. The influence of the impeller size on the mass transfer rates in agitating vessels has been shown by Schindler and Treybal [9]. Brown and Pitt [10, 11] found that the drop size measured at the impeller tip for three different liquid-liquid systems were identical at a given speed of rotation for two impellers of identical diameter but different blade heights. The authors attributed the identical drop diameters to identical turbulent head characteristics in the stream from each impeller. A discussion of the effect of the impeller blade geometry on the drop size is given by Kichatov et al. [12].

A disk turbine type impeller is widely accepted for many liquid-liquid agitation processes. Giapos et al. [13] found that increasing the number of impeller blades of a disk turbine impeller results in a decrease of the drop sizes. Bates et al. [14] found that the power number in an agitated vessel depends also on the impeller blade height. Maynes and Butcher [15] and Kumaresan and Joshi [16] found also that the impeller power number decreases with a decrease in impeller height.

[*] H. Naseef, A. Soultan, M. Stamatoudis (author to whom correspondence should be addressed, stamatou@auth.gr), Department of Chemical Engineering, Aristotle University of Thessaloniki, GR-54124 Thessaloniki, Greece.

1) List of symbols at the end of the paper.

A review of the effect of impeller design on the liquid-liquid mixing is given by Nere et al. [17]. Thus, it is important to study the effect of impeller blade height on the drop sizes at a given impeller rotational speed since no attention has been given in the literature on this important area.

2 Experimental

The experiments were conducted in a closed cylindrical vessel made from glass. It had a 30 cm inside diameter. The ends were a little wider due to the existence of a very slight flair. The height was 30.5 cm. The top and the bottom plates of the vessel were made of aluminum. The vessel was provided with four equally spaced vertical baffles each being 3 cm wide. A 3.9 cm inside diameter cylinder was fitted on the top plate of the vessel. The impeller shaft was inserted through this cylinder. The purpose of this cylinder was to keep the liquid level 2–3 cm above the liquid level inside the vessel in order to prevent air entrainment. A schematic drawing of this experimental apparatus is showed in Fig. 1. The impeller used (shown in Fig. 2) was positioned in the center of the vessel. Four flat vertical six-blade disk style impellers (D = 10 cm, $D_L = D/4$, $D_d = 2/3D$, x_d = 0.15 cm, x_b = 0.12 cm) were used. They differed only in the blade height (D_W = 1, 2, 4, and 6 cm). A 0.37 kW agitator (type Rd 10.12 V, FLUID, Germany) having a variable speed drive, was used to move the 2.5 cm diameter impeller shaft. A Julabo PC circulator was used to circulate water through a coil inserted into the vessel. This was undertaken in order to maintain the vessel liquids at 25 ± 0.1 °C.

The dispersion had distilled water as the continuous phase and kerosene as the dispersed phase. The dispersed phase had a viscosity of μ = 0.00174 Pa·s (measured by a Cannon-Fenske viscometer), a density of ρ = 0.79 g/cm^3, and an interfacial tension of σ = 0.032 N/m (measured by a Du Nouy

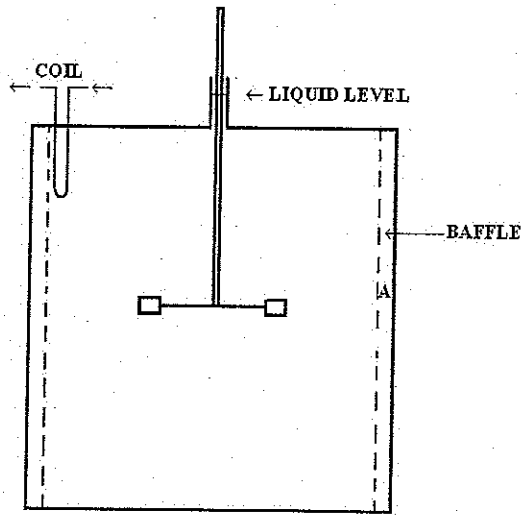

Figure 1. Schematic diagram of the stirred vessel.

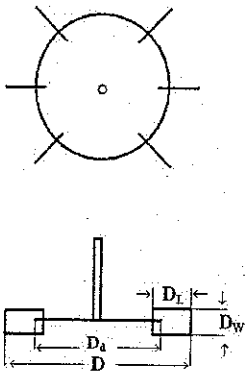

Figure 2. Schematic diagram of a disk type impeller.

type tensiometer). Measurements were made at dispersed holdup fractions ϕ = 0.02, 0.05, and 0.07. Experiments were conducted at impeller rotational speeds N = 200, 250, 300, 350, 400, and 450 rpm. The impeller Reynolds number, N_{Re}, was greater than 30 000 for all experiments. The impeller rotational speed was measured by a 725 DIGI-BETA stroboscope (made by Mayer and Wonisch, Germany). The lower rotational speed limit depended on the impeller height and on the dispersed phase holdup fraction. The purpose was to produce enough agitation to result in the dispersion of all of the organic phase into the water phase.

In situ photomicrography was used to measure the drop size distributions. Photographs were taken at 0.5 cm (position A in Fig. 1) behind the glass wall and 0.25 cm above the center of the vessel. In order to expedite good light illumination, a 2 × 4 cm mirror was attached on a baffle 1.5 cm behind the glass wall where the photographs were taken. Photographs were taken by a camera attached to a Sz-Tr Olympus Zoom Stereo Microscope. In order to "freeze" the high speed moving drops, the camera shutter was kept open and the electronic flash unit (the 725 DIGI-BETA stroboscope described previously) was triggered at prescribed times. The light flashes were directed towards the mirrors and were then reflected back and into the stereoscope. Enough photographs were taken to make samples of at least 500 drops. The slides were projected on a screen and the drop sizes were measured with known magnification. The magnification was found by photographing a wire of known diameter. The maximum errors of the drop diameter measurements were estimated to be around 3.5 %.

3 Results and Discussion

Experimental results for all cases showed that the blade height plays an important role in the drop sizes. Fig. 3 shows the drop distributions for the holdup fraction ϕ = 0.07 and at the rotational speed N = 450 rpm at the four impeller blade heights. From this figure and from others not shown here at other holdup fractions and impeller speeds it is observed that at a given rotational speed and holdup fraction increas-

ing the impeller height results in smaller drops and narrower distributions. This is contrary to the results found by Brown and Pitt [10, 11] who noticed that the drop sizes do not depend on the impeller blade height. This difference may be due to their measurements taken at the impeller tip where breakage predominates while the measurements of the current work were taken further away. Following Bayvel's [18] method a comparison was made of various distribution functions on the ability to describe the experimental drop size distributions. The relatively best distribution that fits the experimental distributions of this work was found to be the cumulative upper limit number one. This cumulative drop number distribution [18] is given by:

$$G(a) = \frac{1}{\sigma_d\sqrt{2\pi}} \int_{-\infty}^{\ln a} \exp\left(-\frac{[\ln\{C_1 a\} - (A_{max} - a)]^2}{2\sigma_d^2}\right) d(\ln a) \quad (3)$$

where σ_d is the standard deviation, A_{max} is the upper limit for a (in this work taken as $1.2\,a_{max}$, the largest measured diameter of the sample), C_1 is a constant, and a_{mean} is the mean diameter.

The observed decrease of the drop sizes with the increase of the impeller blade height is expected, as the impeller power number increases with the impeller height as shown by Bates et al. [14] and Brown and Pitt [11]. The increase in the impeller power number results in a greater energy dissipation and, thus, greater drop breakage rates and/or smaller coalescence rates. Another view on this is obtained when looking at the effect of the impeller blade height on the Sauter mean diameter, a_{32}. Fig. 4 shows the plot of $\ln a_{32}$ as a function of $\ln D_W$ for $\phi = 0.07$. From this figure and from the other data for $\phi = 0.02$ and 0.05 (not shown here) it is observed that the decrease of the impeller blade height from $D_W = 6$ cm to 1 cm results in a substantial increase of a_{32} ranging between 47 and 140 %. It is also observed from Fig. 4 that the plots gave straight lines ($R^2 = 0.94$–0.98) for all impeller rotational speeds. Similar results are obtained for $\phi = 0.02$ and 0.05. The slopes of the lines for all holdup fractions ranged from –0.24 to –0.5.

Bates et al. [14] conducted experiments on the effect of impeller blade height on the power number, N_P, and found that for the six blade turbine style impellers:

$$N_P \propto D_W \quad (4)$$

It is known that:

$$\varepsilon \propto N_P \quad (5)$$

For a given impeller diameter and impeller rotational speed, combining Eqs. (2), (4), and (5) results in:

$$a_{max} \propto D_W^{-2/5} \quad (6)$$

Thus, the slopes of the lines shown in Fig. 4 are close to the theoretically derived slope of –0.4 of relation (6).

Fig. 5 shows that the plots of $\ln a_{32}$ vs. $\ln N$ for the four impeller blade heights for $\phi = 0.07$ gave straight lines ($R^2 = 0.97$–0.99) with slopes ranging from –0.62 to –1.3. Rushton et al. [19] and Bates et al. [14] showed that for $N_{Re} > 10000$:

$$\varepsilon \propto N^3 \quad (7)$$

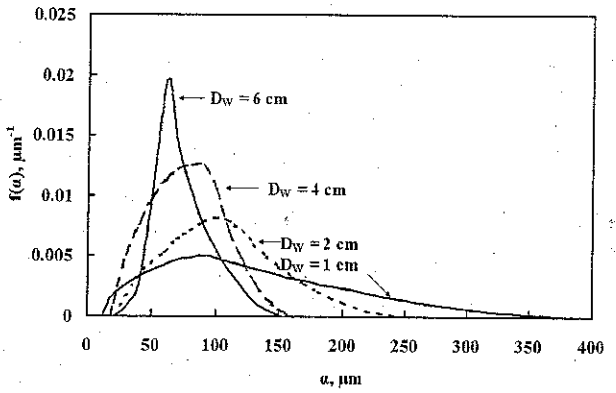

Figure 3. Drop size distributions produced by disk type impellers of various impeller blade heights for $\phi = 0.07$ and $N = 450$ rpm.

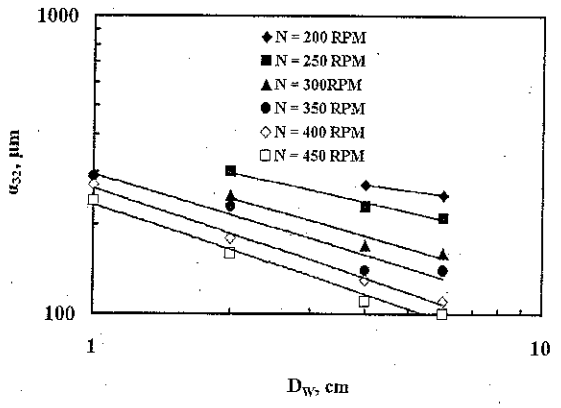

Figure 4. Plots of $\ln a_{32}$ vs. $\ln D_W$ for various impeller rotational speeds and for $\phi = 0.07$.

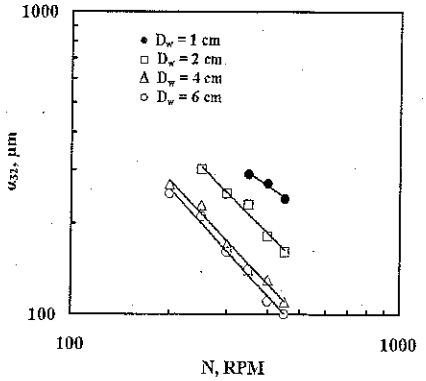

Figure 5. Plots of $\ln a_{32}$ vs. $\ln N$ for the four impeller blade heights for $\phi = 0.07$.

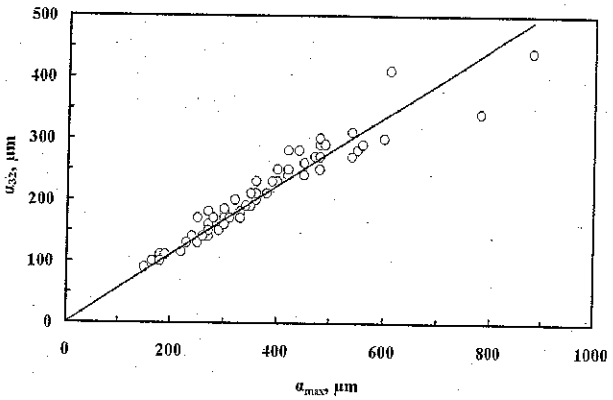

Figure 6. Plots of a_{32} vs. a_{max} for all holdup fractions, impeller speeds, and impeller blade heights studied in the present work.

By combining Eqs. (2) and (7), the following is obtained:

$$a_{max} \propto N^{-6/5} \quad (8)$$

Thus, the slopes of the lines in Fig. 5 are close to the theoretical –1.2 of relation (8).

Fig. 6 shows that the plot of a_{32} vs. a_{max} for all impeller blade heights, impeller rotational speeds, and holdup fractions gave straight lines (R^2 = 0.9) with a slope of 0.56. It should be noticed that the line was forced to pass through the origin. Experiments conducted by Sprow [20] and Brown and Pitt [21] with disk impellers showed slopes of 0.38 and 0.70, respectively. Van Heuven and Hoevenaar [22] and Giles et al. [23] found values of 0.50 and 0.65, respectively. On the other hand, experiments conducted at very low holdup fractions (ϕ = 0.0003) by Zhou and Kresta [24] showed that the relationship a_{32} vs. a_{max} was not quite linear, even though the slope did not change significantly (0.42–0.69).

4 Conclusions

The drop diameters produced by four disk type impellers differing only in their blade height and at different rotational speeds were investigated. Experiments were conducted in an agitated vessel at ϕ = 0.02, 0.05, and 0.07 and at rotational speeds of 200, 250, 300, 350, 400, and 450 rpm. Decreasing the impeller blade height resulted in wider drop distribution curves. The distribution curves were described well by the cumulative upper limit function. Plots of $\ln a_{32}$ vs. $\ln N$ gave straight lines for all blade heights with slopes ranging between –0.62 and –1.3. Plots of $\ln a_{32}$ as a function of $\ln D_W$ gave straight lines with slopes ranging from –0.24 to –0.5 which is in agreement with the theory for isotropic agitated dispersions. Plots of $\ln a_{32}$ vs. $\ln a_{max}$ for all experiments conducted in this work gave a straight line with a slope of 0.56.

Received: April 15, 2005

Symbols used

A_{max}	[µm]	constant of Eq. (3) (taken here as 1.2 a_{max})
C_1	[–]	constant of Eq. (3)
D	[cm]	impeller diameter
D_d	[cm]	disk diameter
D_L	[cm]	length of impeller blade
D_W	[cm]	height of impeller blade
$f(a)da$	[–]	number fraction of drops of diameter between a and $(a + da)$
$G(a)$	[–]	the cumulative upper limit distribution function (defined in Eq. (3))
n_i	[–]	number of drops of diameter a_i
N	[min^{-1}]	impeller rotational speed
N_P	[–]	impeller power number, $P/\rho N^3 D^5$
N_{Re}	[–]	impeller Reynolds number, $ND^2\rho/\mu$
N_{We}	[–]	Weber number, $D^3N^2\rho/\sigma$
P	[J/s]	impeller power
x_d	[cm]	disk thickness
x_b	[cm]	blade thickness

Greek symbols

a	[µm]	drop diameter
a_i	[µm]	drop diameter in the interval i
a_{max}	[µm]	experimental maximum diameter
a_{mean}	[µm]	experimental mean diameter
a_{32}	[µm]	Sauter mean diameter $(\Sigma n_i a_i^3)/(\Sigma n_i a_i^2)$
ε	[J/kg s]	rate of energy dissipating per unit mass of liquid
ϕ	[–]	holdup fraction (m^3 of dispersed phase/m^3 of dispersion)
μ	[Pa s]	viscosity
ρ	[kg/m^3]	density
σ	[N/m]	interfacial tension
σ_d	[µm]	standard deviation

References

[1] L. L. Tavlarides, M. Stamatoudis, *Adv. Chem. Eng.* **1981**, *11*, 199.
[2] A. N. Kolmogoroff, *Dokl. Akad. Nauk. SSSR* **1949**, *66*, 825.
[3] J. O. Hinze, *AIChE J.* **1955**, *1*, 289.
[4] F. B. Sprow, *AIChE J.* **1967**, *13 (5)*, 995.
[5] J. Y. Park, L. M. Blair, *Chem. Eng. Sci.* **1975**, *30*, 1057.
[6] M. Tanaka, *Can. J. Chem. Eng.* **1985**, *63*, 723.
[7] D. Christodoulou, M Stamatoudis, *Can. J. Chem. Eng.* **1991**, *70*, 190.
[8] D. Daglas, M. Stamatoudis, *Chem. Eng. Technol.* **2000**, *23 (5)*, 437.
[9] H. D. Schindler, R. E. Treybal, *AIChE J.* **1968**, *14*, 790.
[10] D. E. Brown, K. Pitt, in *Proc. Chemeca '70*, Melbourne and Sydney **1970**.
[11] D. E. Brown, K. Pitt, *Chem. Eng. Sci.* **1974**, *29*, 345.

[12] B. V. Kichatov, A. M. Korshunov, I. V. Boiko and P. V. Assorova, *Theor. Found. Chem. Eng.* **2003**, *37 (1)*, 19.
[13] A. Giapos, C. Pachatouridis, M.Stamatoudis, *Chem. Eng. Res. Des.* **2005**, *83 (A12)*, 1425.
[14] R. L. Bates, P. L. Fondy, R. R. Corpstein, *Ind. Eng. Chem. Process Des. Dev.* **1963**, *2*, 310.
[15] D. Maynes, M. Butcher, *AIChE J.* **2002**, *48*, 38.
[16] T. Kumaresan, J. B. Joshi, *Chem. Eng. J.* **2006**, *115 (3)*, 173.
[17] N. K. Nere, A. W. Patwardhan, J. B. Joshi, *Ind. Eng. Chem. Res.* **2003**, *42 (12)*, 2661.
[18] L. P. Bayvel, *Atomiz. Spray Technol.* **1985**, *1*, 3.
[19] J. H. Rushton, E. W. Costich, H. J. Everett, *Eng. Prog.* **1950**, *46*, 467.
[20] F. B. Sprow, *Chem. Eng. Sci.* **1967**, *22*, 435.
[21] D. E. Brown, K. Pitt, *Chem. Eng. Sci.* **1972**, *27*, 577.
[22] J. W. van Heuven, J. C. Hoevenaar, in *Proc. 4th Int. Symp. on Reaction Engineering*, Brussels **1969**.
[23] J. P. Giles, C. Hanson, J. G. Marsland, in *Proc. I.S.E.C.*, Amsterdam **1971**.
[24] G. Zhou, S.M. Kresta, *Chem. Eng Sci.* **1998**, *53*, 2063.

